Inorg. Chem. **2007**, *46*, 11213–11223

Rare Examples of Transition-Metal–Main-Group Metal Heterometallic Metal–Organic Frameworks from Gallium and Indium Dipyrrinato Complexes and Silver Salts: Synthesis and Framework Variability

Jay R. Stork, Van S. Thoi, and Seth M. Cohen*

Department of Chemistry and Biochemistry, University of California, San Diego, 9500 Gilman Drive, La Jolla, California 92093-0358

Received August 14, 2007

New main-group metal dipyrrinato complexes [M(4-pyrdpm)$_3$], where M = Ga^{3+} or In^{3+} and 4-pyrdpm is the anion of 5-(4-pyridyl)dipyrrin (4-pyrdpmH), have been synthesized and incorporated into metal–organic frameworks (MOFs) by reacting the dipyrrinato complexes with silver(I) salts. MOFs formed with AgOTf (OTf = O_3SCF_3) and $AgSbF_6$ gave frameworks with three-dimensional (10,3) and two-dimensional (6,3) topologies, respectively. In contrast, $AgPF_6$ produced both (10,3) and (6,3) network topologies, suggesting that the PF_6 anion has little preference for templating (10,3) versus (6,3) frameworks within this system. These findings update an earlier MOF study that examined the role of these anions in templating related heterometallic MOFs which used [Fe(4-pyrdpm)$_3$] and [Co(4-pyrdpm)$_3$] metalloligands. All of the dipyrrin compounds reported here have been characterized by single-crystal X-ray crystallography, including the first crystallographically characterized example of a 1,2,3-unsubstituted free-base dipyrrin, 4-pyrdpmH.

Introduction

Dipyrrins are bipyrrolic ligands best known as the chromophores in BODIPY dyes (BODIPY = difluoroborondipyrrin).[1−7] Much of the interest in dipyrrin compounds derives from their rich optical properties. Compounds that incorporate dipyrrins are often deeply colored and can display intense photoluminescence. While there are a number of examples of dipyrrin complexes with boron or first-row transition metals, main-group metal dipyrrinato complexes have not been examined to the same extent. With the objective of expanding the chemistry of dipyrrins, we recently reported the synthesis of several indium(III) and gallium(III) dipyrrinato complexes.[8] In the same report, we discussed the potential of incorporating similar complexes into metal−organic frameworks (MOFs).

MOFs comprise a very active area of current research.[9−12] These solid-state compounds generally consist of metal nodes connected by organic linkers into rigid, two- or three-dimensional structures. Large pores are often found in these structures, and the pores can generate surface areas comparable to—and sometimes in excess of—zeolites. It has been demonstrated that such large surface areas can lead to substantial gas storage and separation qualities.[13,14] Although some limited success has been realized in ab initio structure generation, topological control and prediction remain important goals in MOF research. Judicious selection of organic

* To whom correspondence should be addressed. E-mail: scohen@ucsd.edu. Tel: (858) 822-5596. Fax: (858) 822-5598.

(1) Ulrich, G.; Goze, C.; Guardigli, M.; Roda, A.; Ziessel, R. *Angew. Chem., Int. Ed.* **2005**, *44*, 3694−3698.
(2) Baruah, M.; Qin, W.; Basarić, N.; De Borggraeve, W. M.; Boens, N. *J. Org. Chem.* **2005**, *70*, 4152−4157.
(3) Baruah, M.; Qin, W.; Vallée, R. A. L.; Beljonne, D.; Rohand, T.; Dehaen, W.; Boens, N. *Org. Lett.* **2005**, *7*, 4377−4380.
(4) Basarić, N.; Baruah, M.; Qin, W.; Metten, B.; Smet, M.; Dehaen, W.; Boens, N. *Org. Biomol. Chem.* **2005**, *3*, 2755−2761.
(5) Qin, W.; Baruah, M.; Stefan, A.; Van der Auweraer, M.; Boens, N. *ChemPhysChem* **2005**, *6*, 2343−2351.
(6) Qin, W.; Baruah, M.; Van der Auweraer, M.; De Schryver, F. C.; Boens, N. *J. Phys. Chem. A* **2005**, *109*, 7371−7384.
(7) Zeng, L.; Miller, E. W.; Pralle, A.; Isacoff, E. Y.; Chang, C. J. *J. Am. Chem. Soc.* **2006**, *128*, 10−11.
(8) Thoi, V. S.; Stork, J. R.; Magde, D.; Cohen, S. M. *Inorg. Chem.* **2006**, *45*, 10688−10697.
(9) Eddaoudi, M.; Moler, D. B.; Li, H.; Chen, B.; Reineke, T. M.; O'Keeffe, M.; Yaghi, O. M. *Acc. Chem. Res.* **2001**, *34*, 319−330.
(10) Holliday, B. J.; Mirkin, C. A. *Angew. Chem., Int. Ed.* **2001**, *40*, 2022−2043.
(11) O'Keeffe, M.; Yaghi, O. M. *J. Solid State Chem.* **2005**, *178*, v−vi.
(12) Moulton, B.; Zaworotko, M. J. *Chem. Rev.* **2001**, *101*, 1629−1658.
(13) Rosi, N. L.; Eckert, J.; Eddaoudi, M.; Vodak, D. T.; Kim, J.; O'Keeffe, M.; Yaghi, O. M. *Science* **2003**, *300*, 1127−1130.
(14) Chae, H. K.; Siberio-Pérez, D. Y.; Kim, J.; Go, Y. B.; Eddaoudi, M.; Matzger, A. J.; O'Keeffe, M.; Yaghi, O. M. *Nature* **2004**, *427*, 523−527.

10.1021/ic7016159 CCC: $37.00
Published on Web 11/30/2007

Scheme 1. Synthetic Route to [M(4-pyrdpm)$_3$AgX] MOFs

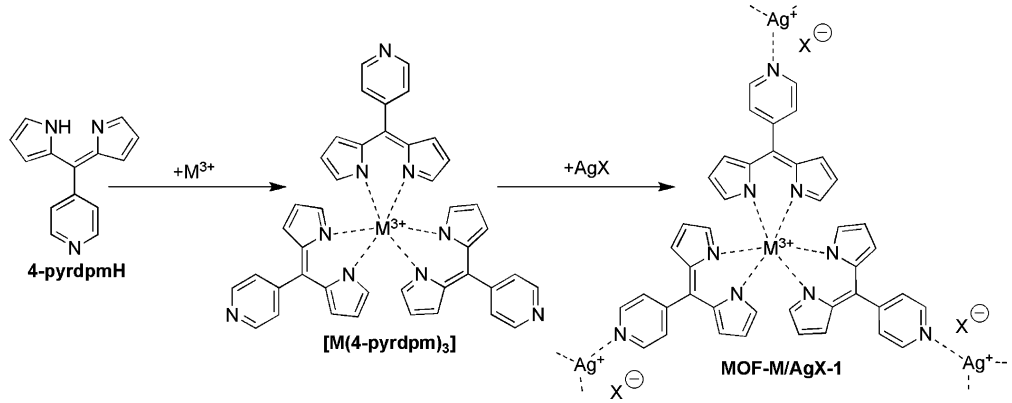

linkers can affect the size of the pores, the extent of interpenetration, and the underlying topology of the framework. Furthermore, the linker can be functionalized to impart desirable physical or catalytic properties to the materials. Because different metal nodes display a wide variety of coordination modes, the choice of metal node also affects the topology and the properties of the material.

In addition to topological control, our interest in MOFs concerns the functionalization of these materials.[15,16] Our approach has been to form MOFs with metalloligands as linkers, thus imparting the functionality of the metalloligand to the MOF material. We have previously reported the synthesis of several MOFs that incorporate silver atoms as nodes and transition-metal dipyrrinato complexes as combined linkers and chromophores.[17−19] The general preparative route toward these MOFs is shown in Scheme 1. The topologies of the resulting frameworks appeared to be profoundly influenced by the counterion.[17,18] In the present report, we describe the synthesis of two new main-group metal dipyrrinato compounds and their incorporation into several MOFs. While the number of reported MOFs has been increasing rapidly in recent years,[20] there are very few MOFs that combine both transition-metal and main-group metal centers. Some transition-metal oxalate complexes have been incorporated into such mixed-metal MOFs,[21−26] and 1,1′-ferrocenedicarboxylic acid has also been used as a constituent of a mixed-metal coordination polymer.[27] MOFs that incorporate both transition and main-group metals are of interest for their electrochemical, catalytic, and luminescence properties. Our new findings, especially concerning the structural variability exhibited by framework compounds that feature PF_6 anions, highlight some limitations in the design of dipyrrinato metalloligand-based MOFs.

Experimental Section

General Procedures. Unless otherwise noted, starting materials were obtained from commercial suppliers and used without further purification. 5-(4-Pyridyl)dipyrromethane was prepared by a literature procedure from freshly distilled pyrrole.[28,29] Tris(5-(4-pyridyl)dipyrrinato)cobalt(III) was synthesized as previously described.[17] Preparative column chromatography was performed on neutral activated alumina (Aldrich, Brockmann activity I) that had been deactivated with 1% H_2O (w/w). Elemental analysis was performed at NuMega Resonance Labs, San Diego, California. ^{1}H/^{13}C NMR spectra were recorded on Varian FT-NMR spectrometers at the Department of Chemistry and Biochemistry, University of California, San Diego. Infrared spectra were collected on a ThermoNicolet Avatar 360 FT-IR instrument. UV−vis spectra were recorded using a Perkin-Elmer Lambda 25 spectrophotometer.

5-(4-Pyridyl)dipyrrin (4-pyrdpmH). 5-(4-Pyridyl)dipyrromethane (0.50 g, 2.25 mmol) was dissolved in 40 mL of $CHCl_3$. 2,3-Dichloro-5,6-dicyano-1,4-benzoquinone (DDQ, 0.52 g, 2.29 mmol) was dissolved in 40 mL of benzene and added dropwise to the $CHCl_3$ solution over the course of 20 min. The mixture was stirred for an additional hour, while monitoring the consumption of dipyrromethane by thin-layer chromatography (neutral alumina; 1:1 CH_2Cl_2/EtOAc). When the reaction appeared to be complete, the solvents were removed on a rotary evaporator to afford approximately 1 g of dark reddish-brown powder. The residue was ground to a powder and suspended in 30 mL of water and was then acidified with 5 mL of 1:10 HCl, forming a blood-red solution with a black precipitate. The solution was filtered through a coarse glass frit and then adjusted to pH ∼8 with 10% KOH. Upon neutralization, the red color was discharged and a yellow suspension formed. The aqueous suspension was extracted with CH_2Cl_2 (4 × 30 mL), and then the combined extracts were washed with saturated $NaHCO_3$. After removal of the solvent, the brown residue was taken

(15) Kitagawa, S.; Kitaura, R.; Noro, S.-I. *Angew. Chem., Int. Ed.* **2004**, *43*, 2334−2375.
(16) Kitagawa, S.; Noro, S.-I.; Nakamura, T. *Chem. Commun.* **2006**, 701−707.
(17) Halper, S. R.; Cohen, S. M. *Inorg. Chem.* **2005**, *44*, 486−488.
(18) Halper, S. R.; Do, L.; Stork, J. R.; Cohen, S. M. *J. Am. Chem. Soc.* **2006**, *128*, 15255−15268.
(19) Murphy, D. L.; Malachowski, M. R.; Campana, C. F.; Cohen, S. M. *Chem. Commun.* **2005**, 5506−5508.
(20) Ockwig, N. W.; Delgado-Friedrichs, O.; O'Keeffe, M.; Yaghi, O. M. *Acc. Chem. Res.* **2005**, *38*, 176−182.
(21) Andrés, R.; Gruselle, M.; Malézieux, B.; Verdaguer, M.; Vaissermann, J. *Inorg. Chem.* **1999**, *38*, 4637−4646.
(22) Chang, W.-M.; Wang, S.-L. *Chem. Mater.* **2005**, *17*, 74−80.
(23) Declercq, J. P.; Feneau-Dupont, J.; Ladriere, J. *Polyhedron* **1993**, *12*, 1031−1037.
(24) Declercq, J. P.; Feneau-Dupont, J.; Ladriere, J. *Polyhedron* **1995**, *14*, 1943−1952.
(25) Decurtins, S.; Schmalle, H. W.; Schneuwly, P.; Ensling, J.; Gütlich, P. *J. Am. Chem. Soc.* **1994**, *116*, 9521−9528.
(26) Sekine, A.; Otsuka, T.; Ohashi, Y.; Kaizu, Y. *Acta Crystallogr., Sect. C* **1994**, *C50*, 1399−1401.
(27) Guo, D.; Mo, H.; Duan, C.-Y.; Lu, F.; Meng, Q.-J. *J. Chem. Soc., Dalton Trans.* **2002**, 2593−2594.
(28) Rao, P. D.; Dhanalekshmi, S.; Littler, B. J.; Lindsey, J. S. *J. Org. Chem.* **2000**, *65*, 7323−7344.
(29) Gryko, D.; Lindsey, J. S. *J. Org. Chem.* **2000**, *65*, 2249−2252.

Table 1. Crystal Data and Data Collection Parameters for 4-pyrdpmH, [Ga(4-pyrdpm)$_3$], and [In(4-pyrdpm)$_3$·1.5CHCl$_3$]

	4-pyrdpmH	Ga(4-pyrdpm)$_3$	In(4-pyrdpm)$_3$·1.5CHCl$_3$
formula	$C_{14}H_{11}N_3$	$C_{42}H_{30}GaN_9$	$C_{43.5}H_{31}Cl_{4.5}InN_9$
fw	221.26	730.47	954.12
cryst syst	monoclinic	monoclinic	triclinic
space group	$P2_1/n$ (No. 14)	$P2_1/c$ (No. 14)	$P\bar{1}$ (No. 2)
a, Å	9.3464(7)	8.597(3)	9.234(5)
b, Å	7.1262(5)	28.610(9)	12.938(7)
c, Å	16.1120(11)	14.372(5)	17.913(9)
α, deg	90	90	82.101(9)
β, deg	92.993(3)	107.716(5)	83.023(9)
γ, deg	90	90	74.558(9)
V, Å^3	1071.66(13)	3367.4(19)	2035.1(18)
Z	4	4	2
T, K	100(2)	100(2)	100(2)
λ, Å	1.54178 (Cu Kα)	0.71073 (Mo Kα)	0.71073 (Mo Kα)
reflns measured	8531	28 597	21 925
independent reflns [R(int)]	1914 [0.0257]	6865 [0.0592]	8256 [0.0281]
D, g/cm^3	1.371	1.441	1.557
μ, mm^{-1}	0.666	0.865	0.922
R1 [$I > 2\,\sigma(I)$][a]	0.0329	0.0493	0.0364
wR2 (all data, F^2 refinement)	0.0912	0.1021	0.0922
GOF on F^2	1.030	1.057	1.057

[a] $R1 = \sum||F_o| - |F_c||/\sum|F_o|$, $wR2 = \{\sum[w(F_o^2 - F_c^2)^2]/\sum[wF_o^4]\}^{1/2}$.

Table 2. Crystal Data and Data Collection Parameters for [Ga(4-pyrdpm)$_3$AgX] MOFs

	MOF-Ga/AgOTf-1b	MOF-Ga/AgOTf-1b′	MOF-Ga/AgPF$_6$-1d	MOF-Ga/AgPF$_6$-1b*	MOF-Ga/AgSbF$_6$-1
formula	$C_{43}H_{30}AgF_3GaN_9O_3S$	$C_{43.19}H_{30}AgF_3GaN_{9.10}O_3S$	$C_{42}H_{30}AgF_6GaN_9P$	$C_{42}H_{30}AgF_4GaN_9P$	$C_{43.85}H_{30}AgF_6GaN_{9.70}Sb$
fw	987.41	991.10	983.31	945.31	1106.12
cryst syst	monoclinic	monoclinic	orthorhombic	monoclinic	triclinic
space group	$C2/c$ (No. 15)	$C2/c$ (No. 15)	$Pbcn$ (No. 60)	$C2/c$ (No. 15)	$P\bar{1}$ (No. 2)
a, Å	30.55(2)	33.3744(17)	27.172(18)	30.705(6)	13.339(3)
b, Å	13.082(9)	66.686(3)	12.563(8)	12.857(3)	16.060(4)
c, Å	33.62(2)	14.9678(8)	33.70(2)	33.146(7)	16.380(4)
α, deg	90	90	90	90	108.941(4)
β, deg	114.739(8)	110.0580(10)	90	116.457(3)	98.464(4)
γ, deg	90	90	90	90	111.852(4)
V, Å^3	12203(14)	31292(3)	11505(13)	11715(4)	2933.5(12)
Z	8	24	8	8	2
T, K	100(2)	100(2)	100(2)	100(2)	100(2)
λ, Å	0.71073 (Mo Kα)	0.71073 (Mo Kα)	0.71073 (Mo Kα)	0.71073 (Mo Kα)	0.71073 (Mo Kα)
reflns measd	71 286	97 520	69 660	35 576	27 016
independent reflns [R(int)]	13380 [0.0811]	31 905 [0.0648]	11 739 [0.0890]	11 900 [0.0506]	11 865 [0.0292]
D, g/cm^3	1.075	1.262	1.135	1.072	1.252
μ, mm^{-1}	0.841	0.985	0.887	0.864	1.296
R1 [$I > 2\sigma\,(I)$][a]	0.0787	0.0496	0.0713	0.0505	0.0642
wR2 (all data, F^2 refinement)	0.2489	0.1202	0.2013	0.1280	0.1905
GOF on F^2	1.063	0.870	0.977	0.893	1.071

[a] $R1 = \sum||F_o| - |F_c||/\sum|F_o|$, $R2 = \{\sum[w(F_o^2 - F_c^2)^2]/\sum[wF_o^4]\}^{1/2}$. * See **Note Added in Proof**.

up in 2 mL of $CHCl_3$ and chromatographed on neutral alumina (15 g) using $CHCl_3$ as eluant. Evaporating the solvent and drying overnight (12 h) in a 50 °C vacuum oven produced the product as a mixture of orange-yellow powder and X-ray-quality crystals that formed by fortuitous sublimation as gold needles. Yield 0.21 g (42%). ^{1}H NMR (400 MHz, $CDCl_3$, 25 °C,): δ 8.72 (AA′BB′ dd, 2H, J = 4.4 Hz, 2.2 Hz, pyH), 7.67 (t, sh, 2H, J = 1.2 Hz), 7.42 (AA′BB′ dd, 2H; J = 4.4 Hz, 2.2 Hz, pyH), 6.52 (dd, 2H, J = 4.2 Hz, 1.0 Hz), 6.41 (dd, 2H, J = 4.0 Hz, 1.6 Hz). ^{13}C NMR (100 MHz, $CDCl_3$, 25 °C): δ 149.5, 145.3, 144.7, 140.2, 138.3, 128.3, 125.3, 118.4. ESI-MS: m/z 222.23 $[M + H]^+$. HR−EI-MS: m/z 221.0951 $[M + H]^+$ (calcd m/z 221.0947). UV−vis (CH_2Cl_2) λ_{max}/nm, (ϵ/M^{-1} cm^{-1}): 434 (20 600), 288 (5200), 244 (6700). IR (thin film): ν 3224, 3101, 3039, 1596, 1574, 1415, 1384, 1354, 1327, 1273, 1252, 1119, 1097, 1047, 1007, 944, 876, 795, 717, 651 cm^{-1}. Anal. Calcd for $C_{14}H_{11}N_3$: C, 76.00; H, 5.01; N, 18.99. Found: C, 76.23; H, 5.35; N, 19.37.

Tris(5-(4-pyridyl)dipyrrinato)gallium(III) ([Ga(4-pyrdpm)$_3$]). Purified 4-pyrdpmH (0.20 g, 0.79 mmol) was dissolved in 14.5 mL of CH_2Cl_2 and 12.5 mL of CH_3OH. To this solution was added 0.25 mL of triethylamine followed by the addition of a solution of $Ga(NO_3)_3$·H_2O (0.13 g, 0.46 mmol) in 2.0 mL of CH_3OH. After stirring overnight and removing the solvents on a rotary evaporator, the orange residue was dissolved in a mixture of CH_2Cl_2 and 0.25% CH_3OH (by volume) and chromatographed on neutral alumina (18 g) with CH_2Cl_2. Removal of the solvent on a rotary evaporator and drying overnight in a 60 °C vacuum oven afforded an orange powder. Yield 0.21 g (96%). ^{1}H NMR (400 MHz, $CDCl_3$, 25 °C): δ 8.70 (AA′BB′ dd, 6H, J = 4.4 Hz, 1.6 Hz, pyH), 7.38 (AA′BB′ dd, 6H; J = 4.4 Hz, 2.0 Hz, pyH), 6.88 (t, sh, 6H, J = 1.4 Hz), 6.55 (dd, 6H, J = 4.0 Hz, 1.2 Hz), 6.30 (dd, 6H, J = 4.0 Hz, 1.6 Hz). ^{13}C NMR (100 MHz, $CDCl_3$, 25 °C): δ 149.6, 149.1, 146.5, 143.8, 138.5, 132.6, 125.2, 117.4. ESI-MS: m/z 729.97 $[M + H]^+$, 509.29 $[M - L]^+$. HR−FAB-MS: m/z 509.1006 $[M - L]^+$ (calcd m/z 509.1000). UV−vis (CH_2Cl_2) λ_{max}/nm, (ϵ/M^{-1} cm^{-1}): 500 (66 000), 448 (90 100), 358, (12 000), 298 (16 400), 246 (28 000). IR (thin film): ν 3103, 3034, 1595, 1556, 1537, 1446, 1409, 1377, 1339, 1241, 1205, 1174, 1048, 1030, 995, 893, 799, 774, 741, 726, 654, 622 cm^{-1}. Anal. Calcd for $C_{42}H_{31}GaN_9O_{0.5}$: C, 68.22; H, 4.23; N, 17.05. Found: C, 68.77; H, 4.53; N, 17.03. Red plates suitable

Table 3. Crystal Data and Data Collection Parameters for [In(4-pyrdpm)$_3$AgX] and [Co(4-pyrdpm)$_3$AgPF$_6$] MOFs

	MOF-In/AgOTf-1b	MOF-In/AgPF$_6$-1	MOF-In/AgPF$_6$-1b*	MOF-Co/AgPF$_6$-1d
formula	$C_{43}H_{30}AgF_3InN_9O_3S$	$C_{85}H_{60}Ag_2F_{12}In_2N_{18.75}P_2$	$C_{42}H_{30}AgF_6InN_9P$	$C_{42}H_{30}AgCoF_6N_9P$
fw	1032.51	2079.34	1028.41	972.52
cryst syst	monoclinic	triclinic	monoclinic	orthorhombic
space group	*C*2*c* (No. 15)	*P*1 (No. 2)	*C*2*c* (No. 15)	*Pbcn* (No. 60)
a, Å	31.160(15)	13.285(4)	31.835(3)	27.062(7)
b, Å	13.208(7)	16.707(5)	12.8637(12)	13.006(3)
c, Å	34.044(17)	27.366(8)	33.715(3)	33.486(8)
α, deg	90	84.264(6)	90	90
β, deg	114.487(8)	85.449(7)	115.3430(10)	90
γ, deg	90	80.949(9)	90	90
V, Å^3	12751(11)	5956(3)	12478(2)	11786(5)
Z	8	2	8	8
T, K	100(2)	100(2)	100(2)	208(2)
λ, Å	0.71073 (Mo Kα)	0.71073 (Mo Kα)	0.71073 (Mo Kα)	0.71073 (Mo Kα)
reflns measd	54 737	70 752	41 189	81 524
independent reflns [*R*(int)]	13 046 [0.1081]	24 065 [0.0393]	12 712 [0.0505]	12 051 [0.1170]
D, g/cm^3	1.076	1.160	1.095	1.096
μ, mm^{-1}	0.744	0.793	0.756	0.690
R1 [$I > 2\sigma(I)$][a]	0.0828	0.0532	0.0621	0.0801
wR2 (all data, F^2 refinement)	0.2100	0.1562	0.1917	0.2387
GOF on F^2	0.996	1.018	0.947	0.894

[a] $R1 = \sum||F_o| - |F_c||/\sum|F_o|$, $R2 = \{\sum[w(F_o^2 - F_c^2)^2]/\sum[wF_o^4]\}^{1/2}$. * See **Note Added in Proof**.

for single-crystal X-ray diffraction were grown by the vapor diffusion of pentane into a saturated $CHCl_3$ solution of the product.

Tris(5-(4-pyridyl)dipyrrinato)indium(III) ([In(4-pyrdpm)$_3$]). To a solution of 4-pyrdpmH (0.20 g, 0.91 mmol) in 15 mL of CH_2Cl_2 and 13 mL of CH_3OH, 0.25 mL of triethylamine was added followed by a solution of $InCl_3 \cdot xH_2O$ (0.10 g, nominally 0.46 mmol) in 2 mL of CH_3OH. The solution was stirred under N_2 overnight (16 h). The subsequent workup was identical to that for [Ga(4-pyrdpm)$_3$], with the product purified by chromatography on neutral alumina with CH_2Cl_2 (0−0.5% MeOH). Yield: 0.20 g (84%). ^{1}H NMR (400 MHz, $CDCl_3$, 25 °C): δ 8.70 (AA′BB′ dd, 6H, $J = 4.4$ Hz, 1.6 Hz, pyH), 7.37 (AA′BB′ dd, 6H; $J = 4.4$ Hz, 1.2 Hz, pyH), 7.12 (s, br, 6H), 6.56 (dd, 6H, $J = 4.2$ Hz, 1.2 Hz), 6.37 (dd, 6H, $J = 4.4$ Hz, 1.2 Hz). ^{13}C NMR (100 MHz, $CDCl_3$, 25 °C): δ 150.5, 149.0, 147.3, 144.8, 139.9, 134.0, 125.2, 117.7. ESI-MS: *m*/*z* 775.94 $[M + H]^+$, 555.13 $[M - L]^+$. HR−FAB-MS: *m*/*z* 555.0786 $[M-L]^+$ (calcd *m*/*z* 555.0783). UV−vis (CH_2Cl_2) λ_{max}/nm, (ϵ/M^{-1} cm^{-1}): 500 (64 100), 446 (123 000), 352, (12 200), 298 (15 300), 246 (26 700). IR (thin film): ν 3103, 3034, 1592, 1550, 1406, 1375, 1334, 1240, 1203, 1172, 1043, 1028, 991, 891, 798, 774, 741, 725, 651 cm^{-1}. Anal. Calcd for $C_{42}H_{30}InN_9$: C, 65.04; H, 3.90; N, 16.25. Found: C, 64.69; H, 4.04; N, 16.27. Red platelike needles suitable for single-crystal X-ray diffraction grew from the vapor diffusion of pentane into a saturated $CHCl_3$ solution of the product.

[M(4-pyrdpm)$_3$AgX] (M = Co^{3+}, Ga^{3+}, In^{3+}; X = $CF_3CO_2^-$, PF_6^-, SbF_6^-). The previously described method was employed in all cases with minor refinements.[17,18] Generally, in the following order, 1 equiv of a 10.5 mM M(4-pyrdpm)$_3$ solution in benzene, neat benzene, and 1 equiv of a 10.5 mM benzene solution of AgX were placed into a glass test tube. Different benzene volumes were used to obtain mixtures that ranged from 0.65 to 2.00 mM of each reactant in a total volume of 3.0 mL of benzene. At all concentrations, a precipitate formed immediately upon the addition of AgX. This initial precipitate was dissolved by the addition of 1.0−3.0 mL of acetonitrile in 0.5 mL aliquots. The addition of 1.0 mL of acetonitrile per 1.5 mL of stock [Co(4-pyrdpm)$_3$] benzene solution eliminated the initial precipitates and the need for additional acetonitrile. However, reaction mixtures containing [Ga(4-pyrdpm)$_3$] or [In(4-pyrdpm)$_3$] still required additional acetonitrile. The solutions were stored in the dark and left to slowly evaporate. Orange crystals that were unstable to solvent loss grew from all solutions after ∼3−15 days. Although we were able to obtain X-ray crystal structures of the MOFs, the decomposition of the MOF crystals after the removal of the mother liquor precluded further characterization.

Single-Crystal X-ray Crystallographic Studies. Suitable crystals of all compounds were selected and covered with a layer of hydrocarbon oil. Crystals were mounted on nylon loops and placed in a cold N_2 stream on the diffractometer. X-ray data were collected on either a Bruker Apex or a Bruker Apex II diffractometer at 100-(2) K using Mo Kα radiation ($\lambda = 0.71073$ Å; Apex) or Cu Kα radiation ($\lambda = 1.54178$ Å; Apex II). A semiempirical method utilizing equivalents was employed to correct for absorption.[30] With the exception of some disordered solvent molecules, all non-hydrogen atoms were refined anisotropically. All hydrogen atoms were located in a difference map, placed in calculated positions, and included in the refinement as riding atoms. The position of the pyrrole hydrogen atom in 4-pyrdpmH was allowed to refine freely without positional restraints. Additional details of the crystallography are provided in Tables 1−3.

Results

Synthesis and Characterization of the Metalloligands. The ligand 5-(4-pyridyl)dipyrrin (4-pyrdpm) was prepared via the oxidation of the precursor 5-(4-pyridyl)dipyrromethane with DDQ in a benzene−chloroform solution. The product was purified by acidifying the crude material followed by the neutralization of the resulting salt and extraction with dichloromethane. Column chromatography on deactivated neutral alumina served as a final purification step, yielding an analytically pure product. Although the yield was modest (42%), we note that our isolated yield of 4-pyrdpmH is comparable to that of the published yields for other 5-substituted dipyrrins.[31] It is anticipated that the

(30) Sheldrick, G. M. *SADABS* (The semiempirical method used is based on a method of Blessing, R. H. *Acta Crystallogr.* **1995**, *A51*, 33), version 2.10; Bruker AXS, Inc.: Madison, WI, 2004.

(31) Yu, L.; Muthukumaran, K.; Sazonovich, I. V.; Kirmaier, C.; Hindin, E.; Diers, J. R.; Boyle, P. D.; Bocian, D. F.; Holten, D.; Lindsey, J. S. *Inorg. Chem.* **2003**, *42*, 6629−6647.

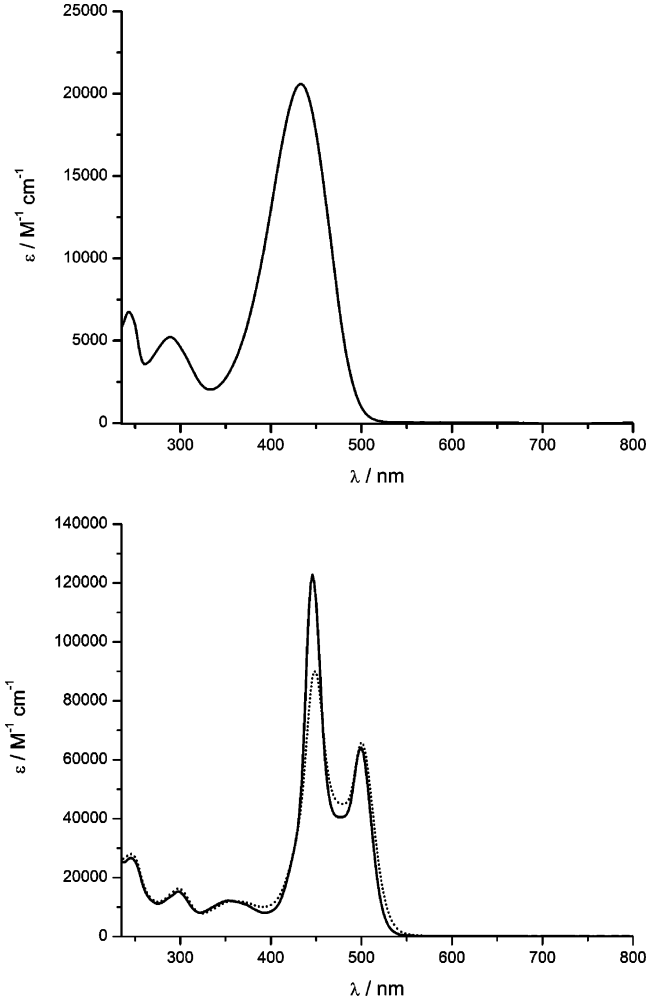

Figure 1. Electronic spectrum of 4-pyrdpmH in dichloromethane solution (top). Electronic spectra of solutions of [Ga(4-pyrdpm)$_3$] (···) and [In(4-pyrdpm)$_3$] (−) in dichloromethane (bottom).

procedure described here may be a general approach for the purification of these free-base dipyrrin compounds.

The metalloligands tris-(5-(4-pyridyl)dipyrrinato)gallium-(III) and tris-(5-(4-pyridyl)dipyrrinato)indium(III) ([Ga(4-pyrdpm)$_3$] and [In(4-pyrdpm)$_3$], respectively) were synthesized by the reaction of purified 5-(4-pyridyl)dipyrrin with either gallium nitrate or indium chloride in a modification of our previously reported method.[17] The compounds were purified by column chromatography on deactivated neutral alumina, which yielded the products in nearly quantitative yield. It is noteworthy that the synthesis of the gallium(III) and indium(III) tris-chelate complexes was greatly facilitated by the use of purified dipyrrin. In our earlier work the dipyrrin purification step was unnecessary, and a crude dipyrrin and dihydroquinone mixture was an acceptable source for the ligand. However, the use of crude intermediates in the synthesis of the present gallium(III) and indium-(III) compounds gave inconsistent results. For instance, an attempt to recrystallize [In(4-pyrdpm)$_3$] that had been prepared from the crude dipyrrin resulted in a 2:1 adduct of [In(4-pyrdpm)$_3$] and dihydroquinone (data not shown).

The electronic spectra of the metal complexes are shown in Figure 1. Both display intense, split, low-energy absorptions as well as several higher-energy processes. The spectra are nearly identical to those of the previously reported 5-(mesityl)dipyrrinato homologues.[8] The low-energy transitions are thus assigned as $\pi \rightarrow \pi^*$ transitions, possibly coupled to a vibrational mode. The split low-energy absorption bands of the gallium(III) and indium(III) complexes contrast with the electronic spectrum of 4-pyrdpmH, which is dominated by a single, unstructured peak at $\lambda_{abs} = 434$ nm (Figure 1).

Crystallographic Studies of the Metalloligands. Gold needles of 4-pyrdpmH were grown by sublimation during drying of the compound in a vacuum oven. The asymmetric unit consists of a single molecule of the dipyrrin. The pyrrole hydrogen atom was found in a difference map and is fully localized on atom N2 (Figure 2). The pyrrole hydrogen atom of dipyrrins is typically believed to be shared between the two pyrrolic nitrogen atoms.[32] However, that assumption is based on the results of solution studies, and in this case, the process of crystallization apparently confines the hydrogen atom to a single pyrrole ring at low temperature. The bonds between the carbon atoms of the dipyrrin skeleton alternate between long and short, ranging from 1.3494(17) Å (C2−C3) to 1.4513(16) Å (C3−C4). The bond-length alternation is more pronounced in the deprotonated ring versus the protonated pyrrole ring. The C−C distances in the protonated ring range from 1.3755(17) Å (C8−C9) to 1.4010(16) Å (C7−C8). This asymmetric bond distribution indicates that the π electrons are only partially delocalized within the dipyrrin moiety in the solid state. Individual 4-pyrdpmH molecules self-associate in the crystal structure to form one-dimensional hydrogen-bonded chains, in which the pyridyl nitrogen atom accepts a hydrogen bond from the pyrrole hydrogen atom. Figure 2 displays a portion of the hydrogen-bonded chain, with selected bond distances and angles given in the caption.

Red, platelike crystals of [Ga(4-pyrdpm)$_3$] were formed by the vapor diffusion of pentane into chloroform solutions of the compound. The structure is free of solvent, and the asymmetric unit contains a single pseudo-octahedral [Ga(4-pyrdpm)$_3$] complex. A drawing of the asymmetric unit is shown in Figure 3. The geometry of the complex is quite similar to that of the previously described [Fe(4-pyrdpm)$_3$] and [Co(4-pyrdpm)$_3$].[17,33] Similarly, red crystals of [In(4-pyrdpm)$_3$] were also grown by the vapor diffusion of pentane into chloroform solutions of the compound. The crystal structure includes one [In(4-pyrdpm)$_3$] complex and 1.5 molecules of chloroform in the asymmetric unit. Although the coordination sphere of the indium(III) ion is pseudo-octahedral, as shown in Figure 3, two of the 4-pyrdpm ligands are canted from their associated N−In−N coordination planes. The plane of the dipyrrin ligand that includes atom N1 makes an angle of 19.83(9)° with the N1−In−N2 coordination plane (Figure 3), while the corresponding angle of the ligand that includes atom N7 is 20.50(9)°. The third such angle, for the ligand that includes atom N4, is 4.42-(12)°.

(32) Wood, T. E.; Thompson, A. *Chem. Rev.* **2007**, *107*, 1831−1861.
(33) Cohen, S. M.; Halper, S. R. *Inorg. Chim. Acta* **2002**, *341*, 12−16.

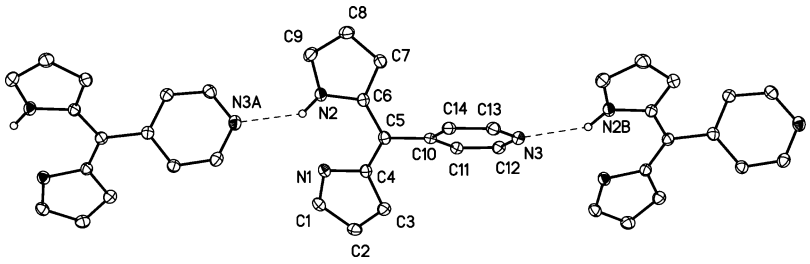

Figure 2. Drawing of a portion of the hydrogen-bonded chain of molecules in 4-pyrdpmH with 50% thermal contours. Most hydrogen atoms have been omitted for clarity. Selected bond distances (Å): C1−N1, 1.3056(16); C1−C2, 1.4437(17); C2−C3, 1.3494(17); C3−C4, 1.4513(16); C4−N1, 1.4071(15); C4−C5, 1.3721(17); C5−C6, 1.4387(16); C5−C10, 1.4865(15); C6−C7, 1.3976(16); C6−N2, 1.3721(15); C7−C8, 1.4010(16); C8−C9, 1.3755(17); C9−N2, 1.3521(16); N2···N3A, 2.9978(14). Selected bond angles (deg): N1−C1−C2, 113.36(10); C3−C2−C1, 105.77(10); C2−C3−C4, 106.52(10); C5−C4−N1, 121.93(10); C5−C4−C3, 128.80(11); N1−C4−C3, 109.21(10); C4−C5−C6, 124.70(11); C4−C5−C10, 119.41(10); C6−C5−C10, 115.84(10); N2−C6−C7, 106.78(10); N2−C6−C5, 124.01(10); C7−C6−C5, 129.08(11); C6−C7−C8, 107.76(10); C9−C8−C7, 106.84(10); N2−C9−C8, 109.04(10).

Crystallographic Studies of the MOFs. The MOFs were grown by the slow evaporation of mixed benzene−acetonitrile solutions of the [M(4-pyrdpm)$_3$] metalloligands and various silver salts, as previously described for a related series of iron(III) and cobalt(III) dipyrrin MOFs.[17,18] In all cases described here, rapid decomposition of the products and a loss of crystallinity accompanies solvent loss. This framework collapse has been previously noted for other MOFs with simple Ag−N nodes.[34] Thus, the compounds were difficult to fully characterize beyond single-crystal X-ray crystallography. All of the MOFs contained large regions of severely disordered solvent molecules, as is common in these open framework compounds. The disordered solvent was treated as a diffuse contribution by application of the *SQUEEZE* program as implemented in *PLATON*.[35] Additionally, most of the MOF structures included disordered anions. The treatments of these sometimes severely disordered anions and solvent molecules are described in the Supporting Information (CIF files). New MOFs prepared from the [In(4-pyrdpm)$_3$] and [Ga(4-pyrdpm)$_3$] metalloligands with various silver(I) salts are shown in Figures 4 and 5 as simplified nodal representations.

[M(4-pyrdpm)$_3$AgOTf]. The frameworks MOF-Ga/AgOTf-1b and MOF-In/AgOTf-1b form as red plates and are isomorphous. They are also nearly identical to the iron congener, although that compound has a doubled unit-cell axis.[18] Because of the similarity of the two new structures, only the structure of MOF-In/AgOTf-1b is described here. The asymmetric unit contains a single [In(4-pyrdpm)$_3$] complex coordinated to a silver(I) ion. A disordered triflate anion near the silver(I) ion completes the charge balance. Pyridyl nitrogens from three separate [In(4-pyrdpm)$_3$] units coordinate the silver ion in a nonequilateral trigonal plane. The Ag−N distances range from 2.248(6) to 2.299(6) Å, and the sum of the N−Ag−N angles is 360(6)°. A very weakly bound triflate anion completes the silver coordination sphere. The nearest Ag−O separation of 2.753 Å is considerably less than the sum of the van der Waals radii (3.24 Å),[36] indicating a fair degree of ionic attraction between the silver(I) and the triflate ions. The doubly interpenetrated, three-dimensional framework consists of alternating [In(4-pyrdpm)$_3$] complexes and silver(I) ions arranged in a (10,3)-b network topology (Schläfli symbol 10^3, vertex symbol $10_2 \cdot 10_4 \cdot 10_4$),[37] as determined with the program *OLEX*[38] and by comparison of the coordination sequence (TD10 = 609) with the Reticular Chemistry Structural Resource database (http://rcsr.anu.edu.au/). Within each of the two frameworks of the lattice are metalloligands of alternating Δ and Λ chirality.

A second structural isomer of [Ga(4-pyrdpm)$_3$AgOTf], dubbed MOF-Ga/AgOTf-1b′, was also obtained. MOF-Ga/AgOTf-1b′ is isomorphic with the previously described MOF-Fe/AgOTf-1. All of these structures, MOF-In/AgOTf-1b, MOF-Ga/AgOTf-1b, MOF-Ga/AgOTf-1b′, and MOF-Fe/AgOTf-1, possess (10,3)-b network topologies. The primary structural differences between MOF-Ga/AgOTf-1b and MOF-Ga/AgOTf-1b′ involve the coordination spheres of the silver(I) ions. MOF-Ga/AgOTf-1b′ includes four independent silver(I) centers (the asymmetric unit includes two full formula units and two half formula units on special positions for a total of three formula units, or $Z' = 3$.) Two of the silver(I) ions have close contacts with the oxygen atoms of triflate anions with closest Ag−O distances that range from 2.611 to 2.652 Å, while the other two silver atoms are more weakly coordinated to triflate anions and have Ag−O distances that range from 2.987 to 3.031 Å. In contrast, MOF-Ga/AgOTf-1b has only one formula unit per asymmetric unit. This arrangement results in a single silver(I) ion associated with a single disordered triflate anion. The Ag−O distances in the latter compound are intermediate between the distances in MOF-Ga/AgOTf-1b′ and range from 2.773 to 2.896 Å. The small geometric differences in MOF-Ga/AgOTf-1b and MOF-Ga/AgOTf-1b′ are manifest in visually distinct arrangements of the (10,3)-b net (Figure 5).

[M(4-pyrdpm)$_3$AgPF$_6$]. The combination of [In(4-pyrdpm)$_3$] and $AgPF_6$ generated two different MOFs, both as red blocks. The structure of MOF-In/$AgPF_6$-1 is isostructural with the previously described MOF-M/$AgPF_6$-1 compounds where M = Fe^{3+} or Co^{3+}.[18] The main residue includes two independent [In(4-pyrdpm)$_3$] complexes that coordinate to two silver(I) ions. Disordered PF_6^- anions and

(34) Abrahams, B. F.; Hoskins, B. F.; Michall, D. M.; Robson, R. *Nature* **1994**, *369*, 727−729.
(35) Spek, A. L. *Acta Crystallogr.* **1990**, *A46* (supplement), C34.
(36) Bondi, A. *J. Chem. Phys.* **1964**, *68*, 441−451.
(37) Öhrström, L.; Larsson, K. *Molecule-Based Materials: The Structural Network Approach*; Elsevier, B. V.: Amsterdam, 2005.
(38) Dolomanov, O. V.; Blake, A. J.; Champness, N. R.; Schröder, M. *J. Appl. Crystallogr.* **2003**, *36*, 1283−1284.

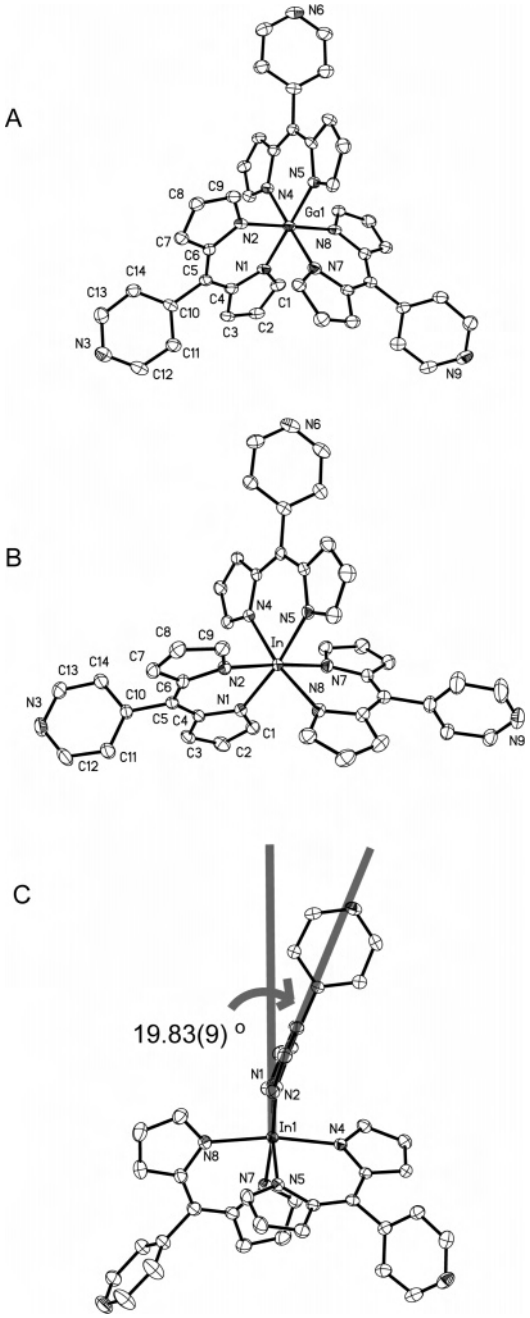

Figure 3. Structures of the complexes (A) [Ga(4-pyrdpm)$_3$] and (B) [In(4-pyrdpm)$_3$] with partial naming schemes and (C) a view of [In(4-pyrdpm)$_3$] emphasizing the out-of-plane coordination geometry of one ligand. The structures are drawn with 50% thermal contours. Selected bond distances (Å): [Ga(4-pyrdpm)$_3$], Ga−N1, 2.062(2); Ga−N2, 2.061-(3); Ga−N4, 2.033(2); Ga−N5, 2.059(2); Ga−N7, 2.058(2); Ga−N8, 2.068(3). [In(4-pyrdpm)$_3$], In−N1, 2.196(2); In−N2, 2.243(2); In−N4, 2.225(2); In−N5, 2.219(2); In−N7, 2.247(2); In−N8, 2.200(2). Selected bond angles (deg): [Ga(4-pyrdpm)$_3$], N1−Ga−N2, 87.82(10); N1−Ga−N5, 176.52(10); N2−Ga−N8, 178.96(10); N4−Ga−N5, 89.00(10); N4−Ga−N7, 177.28(10); N7−Ga−N8, 87.85(10). [In(4-pyrdpm)$_3$], N1−In−N2, 82.83(9); N1−In1−N5, 171.59(8); N2−In−N7, 176.35(8); N4−In−N5, 84.36(8); N4−In−N8, 169.50(8); N7−In−N8, 82.94(9).

solvent make up the remainder of the asymmetric unit. Each silver(I) ion is bound to a pyridyl nitrogen atom of three different indium(III) complexes in a slightly pyramidalized fashion. The sums of the pyridyl N−Ag−N angles are 353.8° and 355.7° for the two silver atoms. Acetonitrile solvent molecules are coordinated to the apical positions of the silver atoms with Ag−N distances of 2.343(4) and 2.332(4) Å. The framework structure consists of two-dimensional sheets that have a (6,3) network topology (Schläfli symbol 6^3 vertex symbol 6·6·6). Each sheet is comprised of homochiral [In-(4-pyrdpm)$_3$] complexes with alternate sheets having opposite chirality, as previously seen in MOF-Fe/AgSbF$_6$-1 and MOF-Co/AgSbF$_6$-1.

Under identical reaction conditions, a second crystalline form was also grown, designated MOF-In/AgPF$_6$-1b. MOF-In/AgPF$_6$-1b is isomorphic with MOF-In/AgOTf-1b and presents a (10,3)-b network topology. The two compounds MOF-In/AgPF$_6$-1 and MOF-In/AgPF$_6$-1b are framework isomers bearing the same counterion. Because of the severely disordered solvent, it is unclear whether the compounds are truly polymorphs in addition to being framework isomers.

Using the [Ga(4-pyrdpm)$_3$] metalloligand in combination with AgPF$_6$ also formed two different structures, as red plates, under the same reaction conditions. Rather than being similar to the previously reported MOF-Fe/AgPF$_6$-1 and MOF-Co/AgPF$_6$-1 structures, the structure of MOF-Ga/AgPF$_6$-1d is isomorphic with MOF-Fe/AgBF$_4$-1 and MOF-Co/AgOTf-1 (Figure 6).[17] That is, MOF-Ga/AgPF$_6$-1d forms with a three-dimensional (10,3)-d network topology (Schläfli symbol 10^3, vertex symbol 10_2·10_4·10_4, TD10 = 621) instead of the two-dimensional (6,3) topology found in MOF-Fe/AgPF$_6$-1, MOF-Co/AgPF$_6$-1, and MOF-In/AgPF$_6$-1. A single [Ga(4-pyrdpm)$_3$] complex coordinated to a silver(I) ion along with a disordered PF$_6$ anion (as well as severely disordered solvent) make up the asymmetric unit. Here again, the silver-(I) ion acts as a trigonal-planar node and is bound to three pyridyl nitrogen atoms with Ag−N bond distances that range from 2.235(5) to 2.244(5) Å. The sum of the N−Ag−N bond angles is 358.5(5)°.

The second structure obtained with [Ga(4-pyrdpm)$_3$] and AgPF$_6$, MOF-Ga/AgPF$_6$-1b, represents another framework isomer. MOF-Ga/AgPF$_6$-1b is isomorphic with MOF-Ga/AgOTf-1b and MOF-In/AgOTf-1b, possessing the (10,3)-b network topology. Although we have not isolated the analogous compound with a two-dimensional (6,3) topology, we cannot rule out its existence, and it seems likely that further crystallization attempts could produce that framework as well.

[Ga(4-pyrdpm)$_3$AgSbF$_6$] (MOF-Ga/AgSbF$_6$-1). MOF-Ga/AgSbF$_6$-1 grows as red plates and is isomorphic with MOF-Fe/AgPF$_6$-1 and MOF-Co/AgPF$_6$-1 from our previous report.[18] The framework has a layered structure with a (6,3) network topology (Figure 6). Like MOF-Fe/AgPF$_6$-1 and MOF-Co/AgPF$_6$-1, each honeycomb layer of MOF-Ga/AgSbF$_6$-1 includes metalloligands of only one chirality, Δ or Λ, and alternate layers have complexes with opposite chirality.

[Co(4-pyrdpm)$_3$AgX] (MOF-Co/AgX-1). Replicating our previously reported syntheses of MOF-Co/AgX-1 compounds with the counterions BF_4^-, OTf^-, and SbF_6^- produced crystals with structures that were identical to our previously reported results.[17,18] However, repeated reactions of [Co(4-pyrdpm)$_3$] with AgPF$_6$ exclusively resulted in the formation

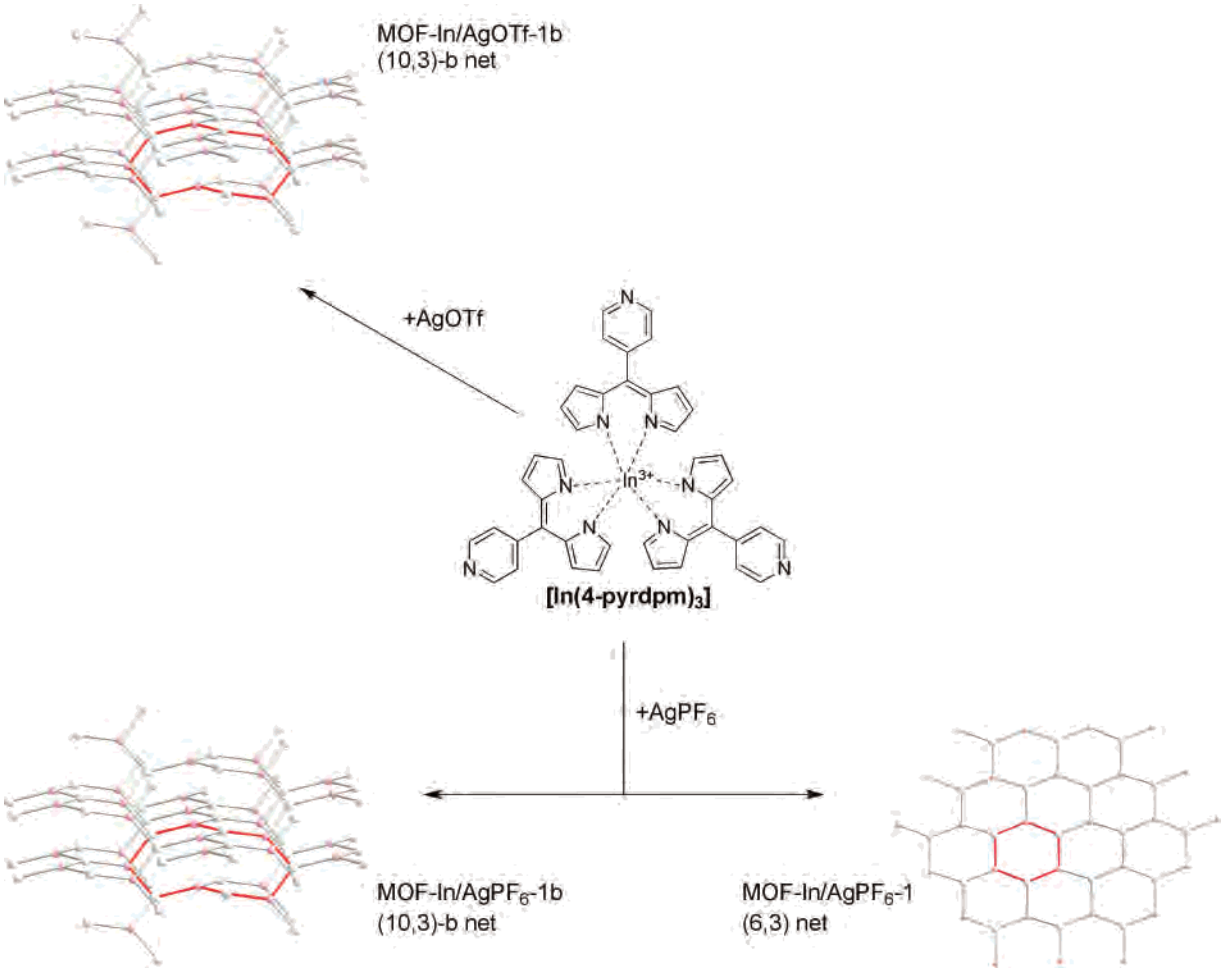

Figure 4. Diagram of MOFs prepared with [In(4-pyrdpm)$_3$]. Indium(III) and silver(I) nodes are shown as pink and gray spheres, respectively. One fundamental circuit is highlighted in red in each example.

of crystals with structures that were isomorphic with MOF-Ga/AgPF$_6$-1d reported here. That is, a new framework isomer, designated MOF-Co/AgPF$_6$-1d, was found which did not have the earlier described (6,3) network topology of MOF-Co/AgPF$_6$-1 from our earlier report, but rather it possessed the same (10,3)-d topology seen in MOF-Ga/AgPF$_6$-1d, MOF-Fe/AgBF$_4$-1, and MOF-Co/AgOTf-1.

Discussion

We began our research into the preparation of MOFs from main-group metal dipyrrinato complexes with two assumptions, both of which later proved to be false. First, the purification of free-base dipyrrins, such as 4-pyrdpmH, via column chromatography was generally inefficient and laborious. Second, the main-group dipyrrinato metalloligands would not be stable to standard column chromatography by virtue of the mostly ionic binding mode between the dipyrrinato ligands and the closed-shell metal centers. Both of these assumptions were based on our prior experience with the syntheses of dipyrrins and main-group dipyrrinato compounds.[8] Over the course of these investigations, it was found that abandoning silica gel in favor of deactivated alumina solved most of the purification challenges for both the dipyrrin and the main-group complexes. This resulted in the development of a better method for isolating 4-pyrdpmH as well as an improved workup procedure for the ensuing metalloligands. Both of the latter methods may find more general utility in the area of dipyrrinato coordination chemistry.[32]

In our initial investigations, we attempted to modify the one-pot procedure for the synthesis of [M(4-pyrdpm)$_3$] (M = Fe^{3+}, Co^{3+}) complexes.[17,18] The original method involved the oxidation of 5-(4-pyridyl)dipyrromethane with DDQ, followed by reaction of the crude dipyrrin with a metal ion source in acetonitrile or mixed chloroform/methanol solutions under reflux. However, the desired complexes, Ga(4-pyrdpm)$_3$ and In(4-pyrdpm)$_3$, did not appear to be stable under those reaction conditions and decomposed during solvent removal, affording uncharacterized black tars.

Three fundamental modifications greatly improved the preparation of the main-group complexes. First, rather than employing crude dipyrrin mixtures in the synthesis of the metal complexes, we opted for a purified dipyrrin source, thus avoiding undesired contaminants. Second, it was found that the indium(III) and gallium(III) complexes formed in excellent yields when allowed to react at room temperature with the pure precursor. Finally, both the dipyrrin precursor and the gallium and indium complexes could be easily

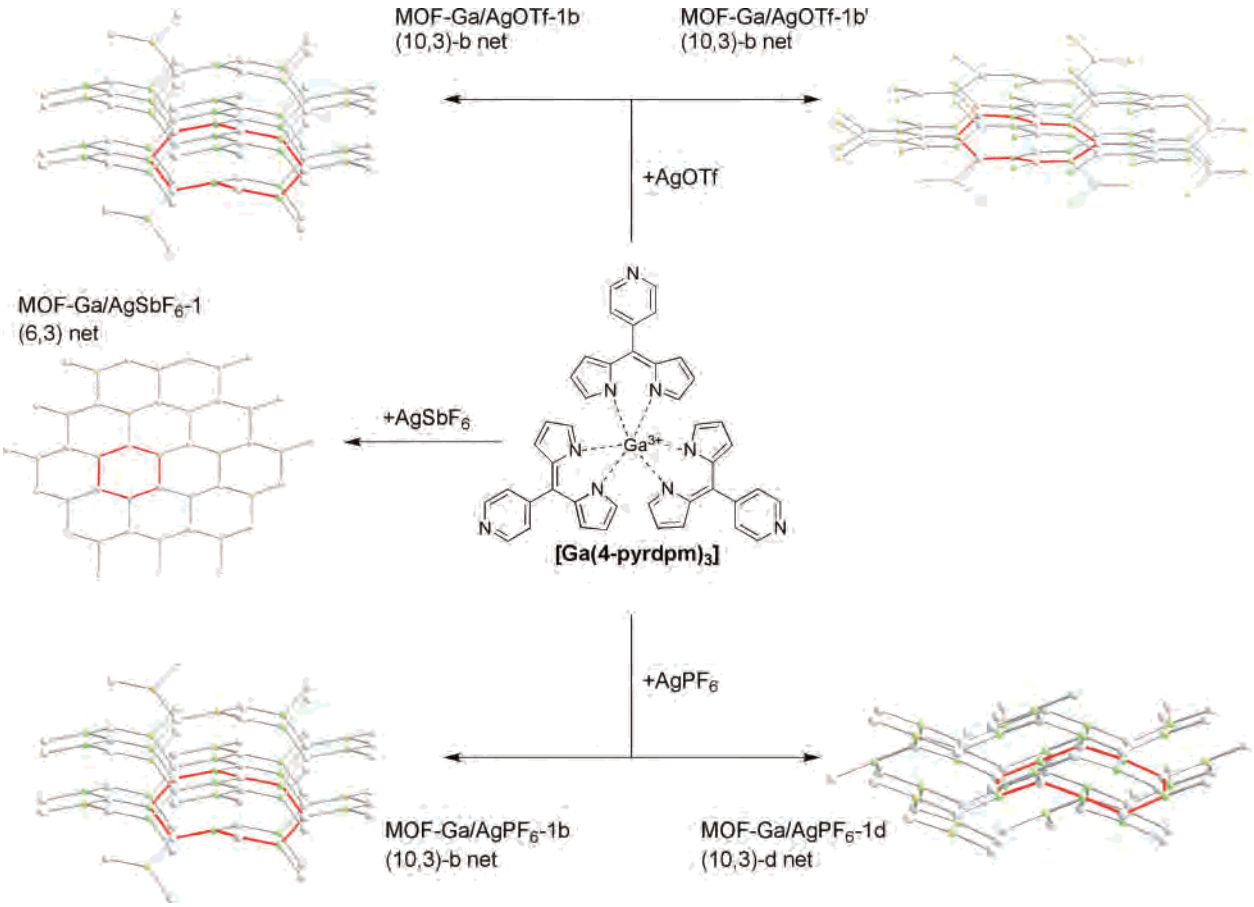

Figure 5. Diagram of MOFs prepared with [Ga(4-pyrdpm)$_3$]. Gallium(III) and silver(I) nodes are shown as green and gray spheres, respectively. One fundamental circuit is highlighted in red in each example.

chromatographed on deactivated neutral alumina to afford pure products. This last finding was particularly important because previous attempts to purify related complexes by silica gel chromatography were unsuccessful.[8]

The network topologies exhibited by the MOFs described here are illustrated schematically in Figures 4 and 5. In earlier reports concerning MOFs that were derived from cobalt and iron tris-dipyrrinato complexes with silver(I) salts, it was found that the choice of counterion in the silver salt appeared to control the ensuing network topologies. Specifically, three-dimensional frameworks with (10,3) network topologies (either (10,3)-b or (10,3)-d) formed when AgOTf or $AgBF_4$ was employed, while syntheses with $AgPF_6$ or $AgSbF_6$ exclusively produced two-dimensional frameworks with (6,3) network topologies. The observation that both MOF-Ga/$AgPF_6$-1b and MOF-In/$AgPF_6$-1b are three-dimensional (10,3) nets encouraged us to re-examine the series of [Co(4-pyrdpm)$_3$AgX] MOFs (MOF-Co/AgX-1, X = BF_4^-, OTf^-, PF_6^-, and SbF_6^-) that we previously reported.[17,18] Repeating the syntheses and structural characterization of the [Co(4-pyrdpm)$_3$]-containing MOFs reproduced our earlier findings with the notable exception of the MOF-Co/$AgPF_6$-1. In our re-examination of this compound, a framework isomer, MOF-Co/$AgPF_6$-1d, consistently formed with a three-dimensional (10,3)-d network topology, instead of the two-dimensional MOF previously found. This result is reminiscent of the finding that the [In(4-pyrdpm)$_3$$AgPF_6$] MOFs reported here can obtain both (10,3)-b and (6,3) network topologies. It appears that the PF_6^- anion can be incorporated de novo in the (10,3) networks of [M(4-pyrdpm)$_3$AgX] MOFs. This is further validated by MOF-Ga/$AgPF_6$-1d and MOF-Ga/$AgPF_6$-1b, which form (10,3)-d and (10,3)-b topologies, respectively. This observation may not be surprising in retrospect, because our earlier ion exchange investigations showed that the PF_6 ion could replace the original OTf ion in a (10,3)-d network without affecting the original topology.[18]

On the basis of the foregoing observations, it is now clear that the anion templating effect that we previously reported does not hold in all circumstances.[18] The network topologies of all of the MOF-M/AgX-1 structures that we have synthesized to date are listed in Table 4. Several tentative observations can be extracted from Table 4: (1) The preference we previously noted[18] among three-dimensional [M(4-pyrdpm)$_3$AgX] frameworks for the (10,3)-d topology over the (10,3)-b topology is belied by the number of (10,3)-b network topologies found in the present work; (2) the OTf and BF_4 anions do seem to instill a bias for (10,3) nets, and the SbF_6 anions seem to instill a bias for (6,3) nets; (3) the PF_6 anion is capable of templating (10,3)-d and (6,3) nets.

The above observations necessarily ignore the contributions of the lattice solvents to the overall stability of the frameworks. This is an unfortunate artifact of the severely disordered solvent molecules in the crystal structures.

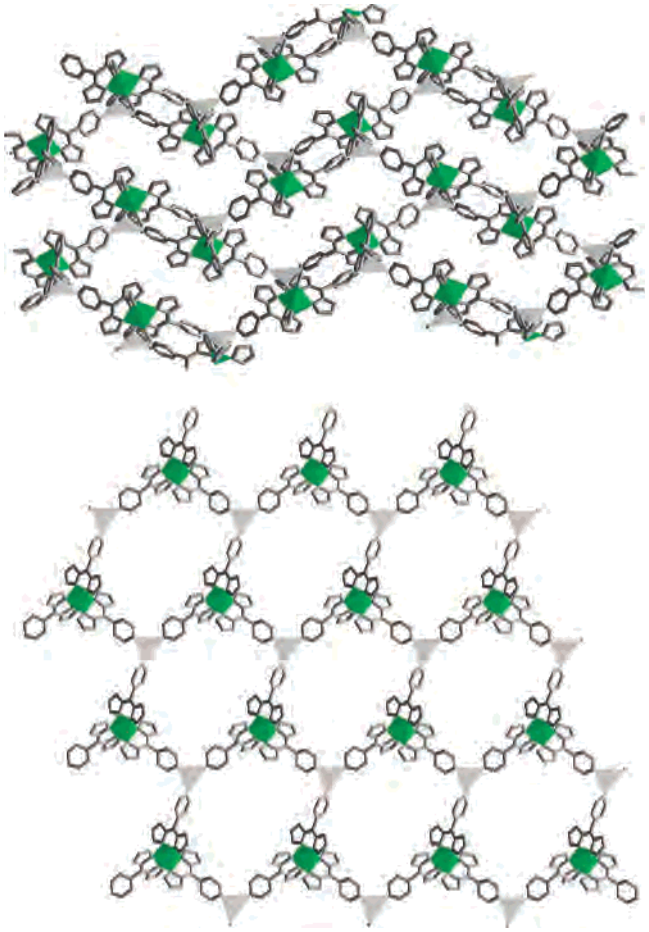

Figure 6. X-ray structures of the (10,3)-d net MOF-Ga/$AgPF_6$-1d (top) and (6,3) net MOF-Ga/$AgSbF_6$-1 (bottom). Gallium(III) and silver(I) centers are shown as green and gray polyhedra, respectively. Hydrogen atoms, anions, and solvent molecules have been omitted for clarity.

Table 4. Network Topologies of [M(4-pyrdpm)$_3$AgX] MOFs

designation	M^{3+}	X^-	space group	network topology
MOF-Co/AgOTf-1[a]	Co	OTf	*Pbcn*	(10,3)-d
MOF-Co/$AgBF_4$-1[b]		BF_4	$P2_1/c$	(10,3)-d
MOF-Co/$AgPF_6$-1[b]		PF_6	$P\bar{1}$	(6,3)
MOF-Co/$AgPF_6$-1d		PF_6	*Pbcn*	(10,3)-d
MOF-Co/$AgSbF_6$-1[b]		SbF_6	$P2_1/c$	(6,3)
MOF-Fe/AgOTf-1[b]	Fe	OTf	$C2/c$	(10,3)-b
MOF-Fe/$AgBF_4$-1[a]		BF_4	*Pbcn*	(10,3)-d
MOF-Fe/$AgPF_6$-1[b]		PF_6	$P\bar{1}$	(6,3)
MOF-Fe/$AgSbF_6$-1[b]		SbF_6	$P2_1/c$	(6,3)
MOF-CoFe/AgOTf-1[b]	Co/Fe	OTf	*Pbcn*	(10,3)-d
MOF-CoFe/$AgBF_4$-1[b]		BF_4	*Pbcn*	(10,3)-d
MOF-Ga/AgOTf-1b	Ga	OTf	$C2/c$	(10,3)-b
MOF-Ga/AgOTf-1b′		OTf	$C2/c$	(10,3)-b
MOF-Ga/$AgPF_6$-1d		PF_6	*Pbcn*	(10,3)-d
MOF-Ga/$AgPF_6$-1b		PF_6	$C2/c$	(10,3)-b
MOF-Ga/$AgSbF_6$-1		SbF_6	$P\bar{1}$	(6,3)
MOF-In/AgOTf-1b	In	OTf	$C2/c$	(10,3)-b
MOF-In/$AgPF_6$-1		PF_6	$P\bar{1}$	(6,3)
MOF-In/$AgPF_6$-1b		PF_6	$C2/c$	(10,3)-b

[a] From ref 17. [b] From ref 18.

Moreover, the number of MOFs analyzed is very limited, and therefore, we cannot rule out the possibility that future efforts will uncover unexpected network topologies. Our new findings also support the possibility that the anion templating effect correlates with the size of the anion. Smaller anions apparently allow for the formation of the generally more dense three-dimensional networks while the largest anion employed, SbF_6, encourages two-dimensional layered structures. Whether this observed effect is related to sterics, charge density, or some other phenomena is as yet unclear. In the case of the PF_6 anion (anion volume of 0.109 nm^3), which has a van der Waals radius intermediate between that of SbF_6 (0.121 nm^3) and the SO_3C moiety ($\sim$0.088 nm^3) of OTf,[39] it is apparent that both (10,3) and (6,3) framework topologies are accessible and that the ensuing network topology is, thus, relatively unpredictable. This caveat is especially significant when one considers that the most obvious structural difference between the (10,3) and the (6,3) networks involves the twisting of the [M(4-pyrdpm)$_3$] complexes away from coplanarity. Although the difference in the geometries is large, there would be little intrinsic barrier to the initial formation of one arrangement over the other, especially when one considers the presence of the intervening silver atom. However, once a crystallization nucleus is formed, the structure will propagate. Thus, as we noted previously, the formation of a framework with a particular network topology likely depends on subtle kinetic and thermodynamic factors.

Conclusion

Two novel main-group metal tris-5-(4-pyridyl)dipyrrinato complexes, [Ga(4-pyrdpm)$_3$] and [In(4-pyrdpm)$_3$], have been synthesized. The purification of the metal complexes using deactivated alumina may be applicable to other dipyrrinato complexes. The syntheses of the metal complexes also incorporated an improved isolation of 5-(4-pyridyl)dipyrrin. The new metal complexes were employed in the synthesis of heterobimetallic, main-group−transition-metal MOFs. All of the present compounds have been characterized by single-crystal X-ray crystallography, including the first crystallographically characterized example of a 1,2,3-unsubstituted free-base dipyrrin.

Except for the MOFs that incorporate $AgPF_6$, these new MOFs are topologically similar and sometimes isomorphic to the previously reported iron(III) and cobalt(III) congeners. Because of the discrepancy between the structures of new [M(4-pyrdpm)$_3$$AgPF_6$] MOFs and previously reported [M(4-pyrdpm)$_3$$AgPF_6$] frameworks, we re-evaluated several [Co(4-pyrdpm)$_3$AgX] structures and discovered a framework isomer of the previously reported structure of MOF-Co/$AgPF_6$-1. These findings prompted reconsideration of the anion templating effect that was formerly postulated. In the modified formulation, it appears that the formation of (10,3) versus (6,3) network topologies in [M(4-pyrdpm)$_3$AgX] compounds is correlated with the anion size. The PF_6 anion, which is intermediate in size among the anions tested, can template either (10,3) or (6,3) nets. Subtle variations in reaction conditions also play a role in determining the ensuing frameworks. It is uncertain at present whether further changes in the reaction conditions will produce additional framework isomers of these MOFs.

Acknowledgment. We thank Prof. Arnold L. Rheingold (U.C.S.D.) for support of the X-ray crystallography facility,

(39) Jenkins, H. D. B.; Roobottom, H. K.; Passmore, J.; Glasser, L. *Inorg. Chem.* **1999**, *38*, 3609−3620.

Dr. Yongshan Su (U.C.S.D.) for performing the mass spectrometry experiments, Prof. David N. Hendrickson (U.C.S.D.) for use of his FT-IR instrument, and Dr. Yilong Yan (U.C.S.D.) for helpful discussions. This work was supported by the University of California, San Diego, the donors of the American Chemical Society Petroleum Research Fund, and the National Science Foundation (CHE-0546531). J.R.S was supported by an NIH training grant (T32 HL007444-25) and V.S.T. was supported, in part, by a U.C.S.D. Summer Research Fellowship.

Note Added in Proof. After acceptance of this manuscript, and because of concerns by one of the reviewers about the disorder of certain hexafluorophosphate anions, we revisited the crystallography of the MOFs prepared with $AgPF_6$. Of the five new MOF-M/$AgPF_6$-1 structures presented herein, we confirmed that three indeed contained the reported PF_6 anions. Those compounds, MOF-Ga/$AgPF_6$-1d, MOF-Co/$AgPF_6$-1d, and MOF-In/$AgPF_6$-1, displayed (10,3)-d, (10,3)-d, and (6,3) network topologies, respectively. However, two compounds MOF-Ga/$AgPF_6$-1b and MOF-In/$AgPF_6$-1b, were found to give better refinement models assuming the inclusion of a PF_2O_2 anion rather than the originally reported PF_6. The origin of PF_2O_2, which is a hydrolysis product of $AgPF_6$, was the $AgPF_6$ starting material that was found to be contaminated, as confirmed by ^{31}P NMR and ^{19}F NMR spectroscopy. A separate CIF file has been provided as Supporting Information to reflect the new formulations. The only compounds that may be affected are MOF-Ga/$AgPF_6$-1b and MOF-In/$AgPF_6$-1b, which both formed two (10,3)-b networks. While this finding does have an impact on the extent of variability in frameworks that contain the PF_6 anion, we maintain that the presence of PF_6 in both (10,3)-d and (6,3) networks, also reported in this paper, is consistent with our statements, on anion templating in both this and earlier reported frameworks. In that prior report, we found that the PF_6 anion could replace trifluoromethanesulfonate (OTf) in (10,3)-d networks without changing the topology.

Supporting Information Available: Complete crystallographic details (CIF file). This material is available free of charge via the Internet at http://pubs.acs.org. X-ray crystallographic files in CIF format are also available free of charge via the Internet at http://www.ccdc.cam.ac.uk. Refer to CCDC reference numbers 657181−657191 and 660729.

IC7016159